Increased Understanding of the Dynamics and Transport in ITB Plasmas from Multi-Machine Comparisons

P. Gohil,[1] J. Kinsey,[2] V. Parail,[3] X. Litaudon,[4] T. Fukuda,[5] T. Hoang[4]

For the ITPA Group on Transport and ITB Physics: J. Connor,[6] E. Doyle,[7] Yu. Esipchuk,[8] T. Fujita,[5] T. Fukuda,[5] P. Gohil,[1] J. Kinsey,[2] S. Lebedev,[9] X. Litaudon,[4] V. Mukhovatov,[10] J. Rice,[11] E. Synakowski,[12] K. Toi,[13] B. Unterberg,[14] V. Vershkov,[8] M. Wakatani,[15] J. Weiland,[16] and for the International ITB Database Working Group: T. Aniel,[4] Yu.F. Baranov,[3] E. Barbato,[17] A. Bécoulet,[4] C. Bourdelle,[4] G. Bracco,[17] R.V. Budny,[12] P. Buratti,[17] E. Doyle,[7] L. Ericsson,[4] Yu. Esipchuk,[8] B. Esposito,[17] T. Fujita,[5] T. Fukuda,[5] P. Gohil,[1] C. Greenfield,[1] M. Greenwald,[11] T. Hahm,[12] T. Hellsten,[3] T. Hoang,[4] D. Hogeweij,[18] S. Ide,[5] F. Imbeaux,[4] Y. Kamada,[5] J. Kinsey,[2] N. Kirneva,[8] X. Litaudon,[4] P. Maget,[4] A. Peeters,[19] K. Razumova,[8] F. Ryter,[19] Y. Sakamoto,[5] H. Shirai,[5] G. Sips,[19] T. Suzuki,[5] E. Synakowski,[12] T. Takizuka,[5] and R. Wolf[19]

[1]General Atomics, P.O. Box 85608, San Diego, California, 92186-5608 USA
email: gohil@fusion.gat.com
[2]Lehigh University, Bethlehem, Pennsylvania 18015 USA
[3]EFDA-JET CSU, Culham Science Centre, Abingdon, Oxon, UK
[4]Association Euratom-CEA, CEA de Cadarache, St Paul lez Durance, France
[5]JAERI, Naka Fusion Research Establishment, Naka, Japan
[6]EURATOM/UKAEA Association, Culham Science Centre, Abingdon, Oxon, UK
[7]University of California, Los Angeles, California 90095 USA
[8]Kurchatov Institute of Atomic Energy, Moscow, Russia
[9]Ioffe Institute, St. Petersburg, Russia
[10]ITER JWS, Naka, Japan
[11]Massachusetts Institute of Technology, Cambridge, Massachusetts 02139 USA
[12]Plasma Physics Laboratory, Princeton University, Princeton, New Jersey 08543 USA
[13]National Institute of Fusion Science, Toki City, Japan
[14]Forschungszentrum Jülich, GmbH, EURATOM-Association, Jülich, Germany
[15]Kyoto University, Kyoto, Japan
[16]Chalmers University and EURATOM-VR association, Gothenburg, Sweden
[17]Associazione EURATOM-ENEA sulla Fusione, C.R. Frascati, Frascati, Italy
[18]FOM Insituut voor Plasmafisica, "Rijnhuizen", Nieuwegein, the Netherlands
[19]Max-Planck-Institut für Plasmaphysik, EURATOM Association, Garching, Germany

Abstract. Our understanding of the physics of internal transport barriers (ITBs) is being furthered by analysis and comparisons of experimental data from many different tokamaks worldwide. An international database consisting of scalar and 2-D profile data on ITB plasmas is being developed to determine the requirements for the formation and sustainment of ITBs and to perform tests of theory-based transport models in an effort to improve the predictive capability of the models. Tests of several transport models (JETTO, Weiland model) using the 2-D profile data indicate that there is only limited agreement between the model predictions and the experimental results for the range of plasma conditions examined for the different devices (DIII–D, JET, JT-60U). Gyrokinetic stability analysis of the ITB discharges from these devices indicates that the ITG/TEM growth rates decrease with increased negative magnetic shear and that the ExB shear rate is comparable to the linear growth rates at the location of the ITB.

1. Introduction

The ITB database variables consist of 134 O-D global and local parameters together with 2-D profile data [e.g., $T_i(r)$, $T_e(r)$, $n_e(r)$, $v_\phi(r)$, $q(r)$, $P_{abs}(r)$]. The scalar part of the database contains more than 1,000 timeslices from many different tokamaks [ASDEX Upgrade, DIII–D, FTU, EFDA-JET, JET, JT-60U, RTP, T10, TFTR, Tore Supra] as well as 4152 profiles in the profile part of the database. Preliminary analysis of the O-D ITB database has focussed on the power threshold for ITB formation based on global variables such as n_e, B_T, and I_p as well as on local quantities such as the magnetic shear at the foot of the barrier [1–3]. In addition, the O-D ITB database has also been used to examine the influence of plasma confinement and magnetic shear on ITB formation [4]. The database has also been used to show that the ratio of the E×B shearing rate, $\omega_{E\times B}$, is comparable to the ion temperature gradient (ITG) growth rate, γ_L, at the time of ITB formation for several devices (JET, JT-60U, TFTR) [5].

2. Predictive Modeling of Plasmas with ITBs

In order to obtain a better understanding of the influence of the *q*-profile on ITB formation, discharges from three major tokamaks (DIII–D, JET, and JT-60U) were modeled using various transport models. Pairs of discharges from each device were selected with one discharge of the pair having a weakly reversed shear or monotonic *q*-profile and the other discharge having a strongly reversed central magnetic shear. Three transport models were used: the JETTO code [6] and the Weiland model [7] and the GLF23 model [8]. In performing the analysis of the above discharges with the GLF23 model, it was determined that the model contained a serious error when modeling discharges with weak or strongly reversed magnetic shear and moderate to large alpha (normalized pressure gradient) [9]. Therefore, the GLF23 model could not be used in this comparative analysis and efforts are underway to correct the model. The JETTO code is based on an empirical mixed Bohm/gyroBohm transport model [10], which has been previously extensively tested on JET plasmas. The Bohm term, which represents the long wavelength part of the turbulence, is suppressed by either a strong E×B shearing rate or by negative magnetic shear such that,

$$\chi_{\mathrm{Bohm}} \propto \frac{|\nabla \mathrm{nT}|}{\mathrm{nB}} \cdot q^2 \cdot \left|\frac{\nabla \mathrm{T_e}}{\mathrm{T_e}}\right|_a \cdot \mathrm{H}\left(0.05 + \mathrm{s} - \mathrm{C} \cdot \frac{\omega_{\mathrm{E\times B}}}{\gamma}\right) \quad , \tag{1}$$

where H(x) is a Heaviside step-function, s is magnetic shear, C is an adjustable numerical factor (of the order of one), γ is the growth rate, $\omega_{\mathrm{E\times B}}$ is the E×B shearing rate. The JETTO model does not include effects of alpha stabilization.

Figures 1 to 3 show the results of predictive modeling of DIII–D, JET and JT-60U discharges using the JETTO code. The experimental profiles of the ion and electron temperatures are compared to the results from the model for different values of the parameter C. The q-profile in the model is evolved in accordance with neoclassical electrical resistivity. The Faraday equation also includes the bootstrap current and any additional current drive from experiment. All neoclassical quantities (e.g. poloidal rotation, resistivity, bootstrap current) are calculated using NCLASS [11]. For the DIII–D discharge with more strongly reversed central magnetic shear (shot 95989), the predicted T_i profile from the model shows reasonable agreement with the experimental profile [Fig. 1(d)] whereas the T_e profile indicates clear underestimation of the temperature by the model [Fig. 1(e)]. There is no significant variation of the modeled temperature profiles with the parameter C since the dominant mechanism for the ITB formation in this model is the negative magnetic shear and the influence of the E×B shearing rate is relatively weak for these conditions. For the case of the weak negative shear discharge (shot 87031), the model substantially overestimates both the T_i and T_e profiles compared to the experimental values [Fig. 1(a,b)]. For the JET discharge with strong negative central shear (shot 53521), there is very good agreement between the model predictions and both the experimental T_i and T_e profiles [Fig. 2(d,e)]. The model provides good agreement with both the absolute value of the central temperature and the spatial location of the transport barrier. However, the model substantially overestimates the temperature profiles for the JET discharge with monotonic *q* profile (shot 46664), particularly the T_i profile [Fig. 2(a)]. This overestimation is very similar to the behavior for weak negative magnetic shear discharges in DIII–D, suggesting that the model is less appropriate for discharges with both weak magnetic shear and strong toroidal rotation or strong pressure gradients. In the case of the JT-60U discharge with monotonic *q* profile (shot 34487), the model clearly fails to reproduce the experimental profiles until the multiplier C exceeds a value of 1.4 [Fig. 3(a)], indicating that the level of experimental toroidal rotation (i.e. E×B shearing rate) in this discharge is too low to trigger the ITB as predicted by the model for the given (i.e. positive) magnetic shear in the plasma. However, if the central magnetic shear is sufficiently negative (shot 39056), the model produces an ion ITB (although not the absolute central ion temperature) without any increased influence from the toroidal rotation and the E×B shearing rate, but again the model fails to produce the electron ITB.

The Weiland model was less successful in reproducing the ITBs when run in predictive simulations. The result of a simulation with the strong negative shear discharge from JET

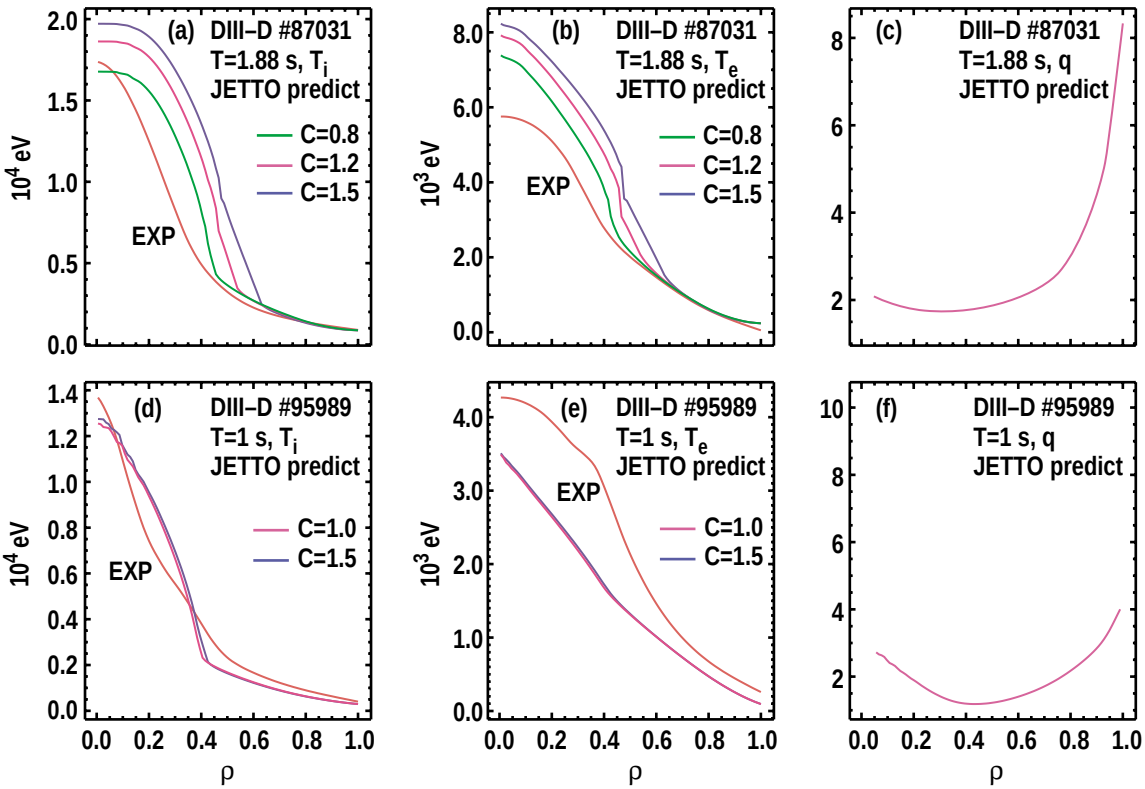

Fig. 1. Comparisons between predicted results from the JETTO transport model and experimental results for the T_i and T_e profiles in ITB discharges in DIII–D. (a–c) correspond to weak negative central magnetic shear; (d–f) correspond to strong negative magnetic shear.

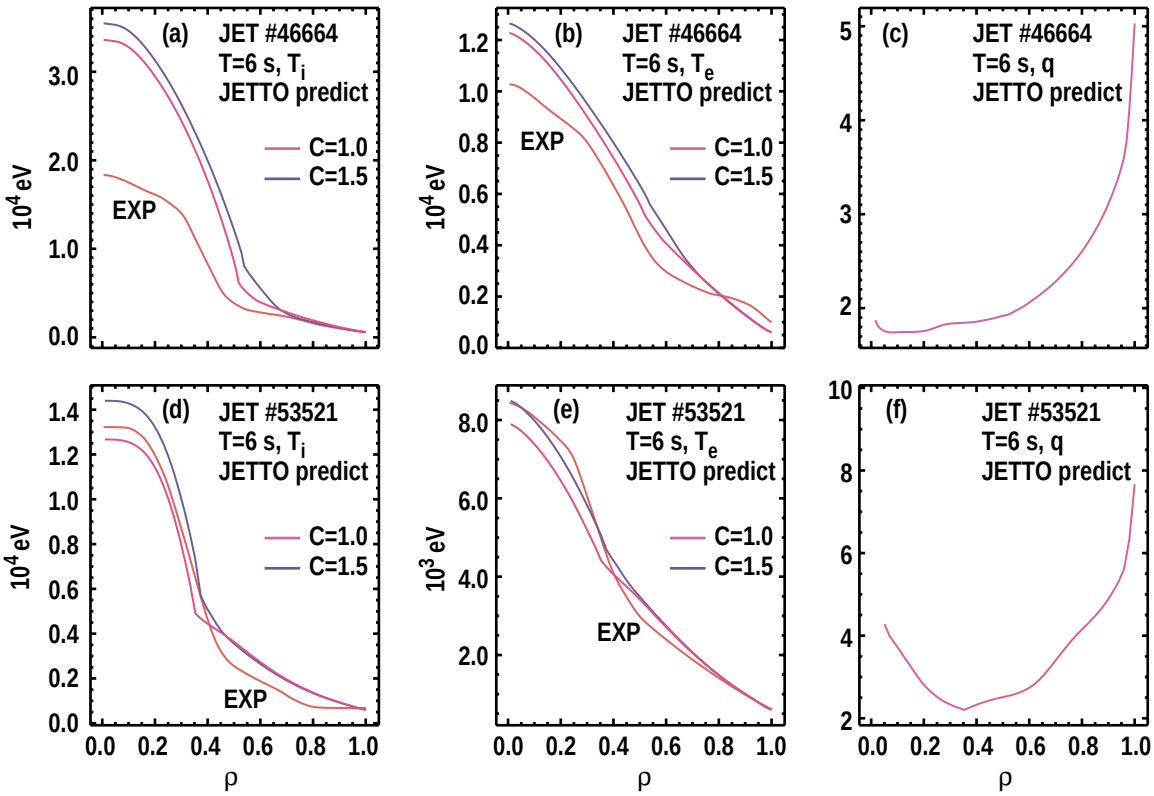

Fig. 2. Comparisons between predicted results from the JETTO transport model and experimental results for the T_i and T_e profiles in ITB discharges in JET. (a–c) correspond to weak positive central magnetic shear; (d–f) correspond to strong negative magnetic shear.

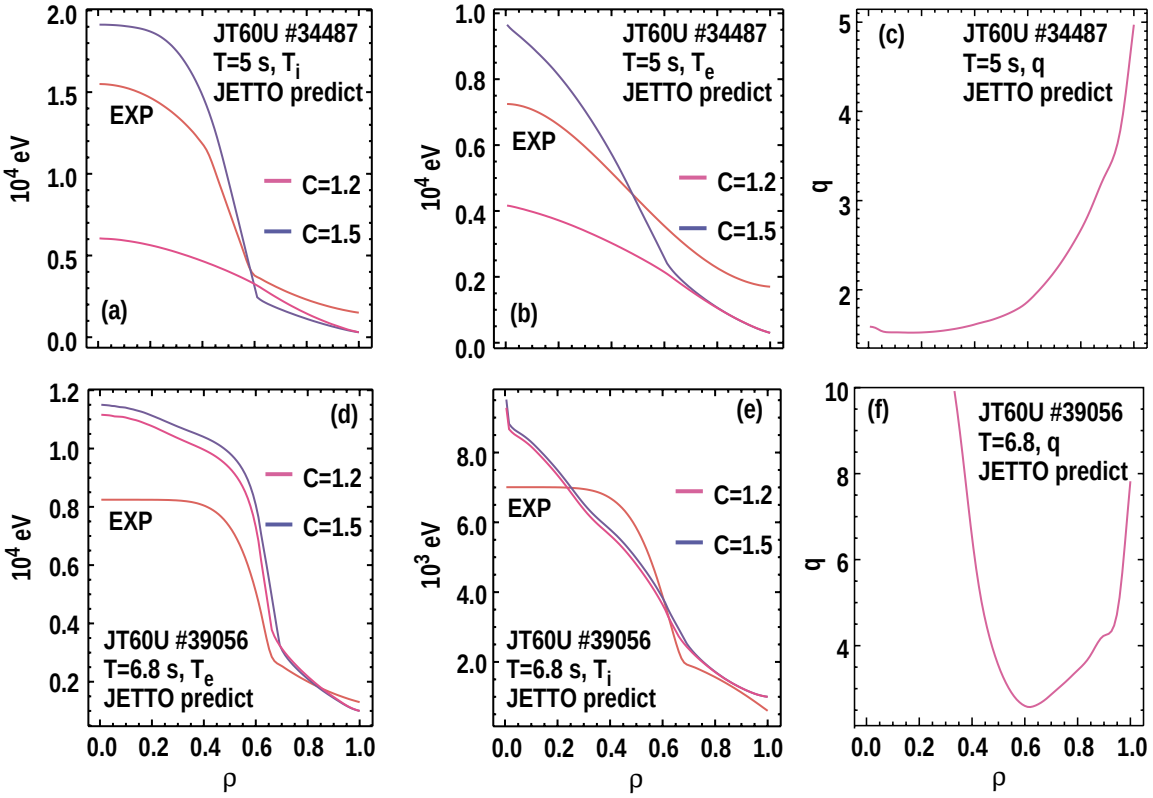

Fig. 3. Comparisons between predicted results from the JETTO transport model and experimental results for the T_i and T_e profiles in ITB discharges in JT-60U. (a–c) correspond to weak positive central magnetic shear; (d–f) correspond to strong negative magnetic shear.

(shot 53521) is shown in Fig. 4. The simulation results do not agree with the experimental data for both the T_i and T_e profiles. Improved agreement is obtained for the T_i profile if the toroidal rotation (and, hence, the E×B shearing rate) is increased by a factor of 4 or, similarly, if the ITG growth rates are reduced by a factor of 4. However, this increase then overestimates the T_e profile. This lack of agreement may be due to the treatment of the E×B flow shear suppression in the model.

3. Gyrokinetic Stability Analysis of ITB Plasmas

The gyrokinetic stability analysis of ITB discharges was also carried out for the six discharges from DIII–D, JET, and JT-60U. The maximum linear ITG/TEM mode growth

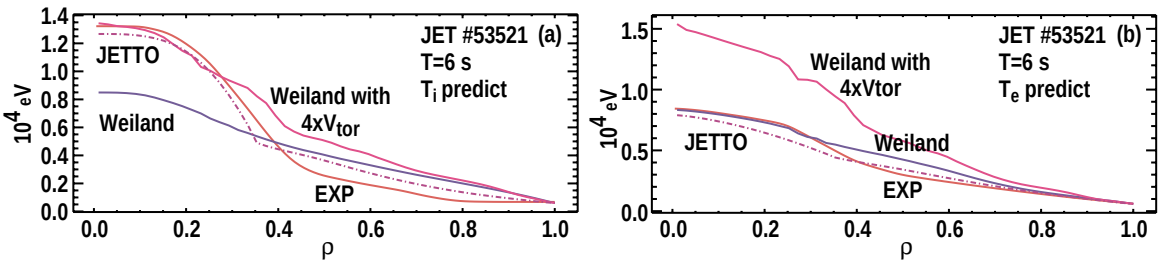

Fig. 4. Comparisons between the predicted values of the the T_i and T_e profiles from the JETTO and Weiland models compared to the experimental results for JET discharge 53521. (a) for the T_i profile and (b) for the T_e profile.

rates were obtained using the GKS gyrokinetic code [12] including non-circular geometry. Fig. 5 shows γ_{max} versus normalized radius for each of the six cases along with the computed E×B shear rate, $\omega_{E\times B}$, evaluated using the formulation of Hahm-Burrell [13] and Waltz [8]. Here, $\omega_{E\times B}$ was computed taking the toroidal rotation and pressure gradient from experimental data and computing the poloidal rotation from neoclassical theory to construct

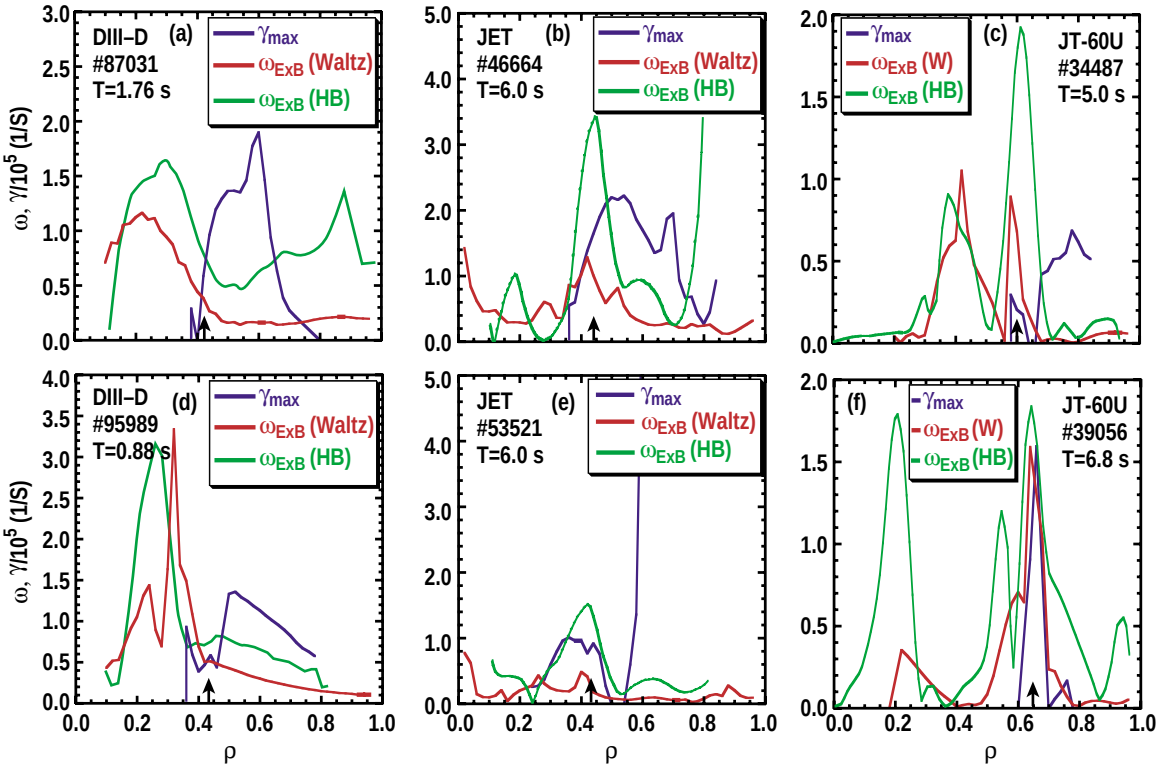

Fig. 5. Comparisons between the radial profiles of the E×B shearing rate and the ITG/TEM growth rates for weak negative/positive magnetic shear (a–c) and strong negative magnetic shear (d–f) in DIII–D, JET and JT-60U. The upward black arrows mark the location of the T_i ITB.

the radial electric field E_r in the radial force balance equation. While E×B shear is effective in suppressing the long wavelength (low-k) ITG growth rates, alpha stabilization (Shafranov shift) is effective in suppressing both the low-k ITG and high-k ETG modes by reducing the geodesic curvature drive for weak or reversed magnetic shear conditions. Shafranov shift can also lead to suppression of TEM modes via drift reversal but TEM modes were not found to be important in the cases examined here with the exception of JET discharge 53521 at ρ=0.6. In general, we find that the magnitude of the ITG mode growth rates near the half-radius are significantly lower for the NCS discharges compared to the monotonic *q*-profile discharges. The requirement for the level of heating and momentum input then needed to produce an ITB is therefore reduced for reversed magnetic shear conditions. The gyrokinetic stability analysis shows that the E×B shear rate is comparable to the maximum linear growth rate for drift-wave instabilities at the location of the ITB.

Work supported by U.S. Department of Energy under Contracts DE-AC03-99ER54463, DE-AC02-76CH03073, and Grants DE-FG03-01ER54615, DE-FG02-92ER54141, DE-FC02-99ER54512.

[1] T. Fukuda, *et al*., Proc. 28th EPS Conference, Maderia, Spain (2001).
[2] A.C.C. Sips, et al., Plasma Phys. Control. Fusion **44**, A391 (2002).
[3] Y. Baranov, Bull. Am. Phys. Soc. **46**, 117 (2001).
[4] G.T. Hoang, *et al*., Proc. 29th EPS Conference, Montreux, Switzerland (2002).
[5] T. Fukuda, *et al*., Proc. 29th EPS Conference, Montreux, Switzerland (2002).
[6] G. Cennachi and A. Tami, JET-IR(88), 03 (1988).
[7] J. Weiland, "Collective Modes in Inhomogeneous Plasmas," Institute of Physics Publishing, Bristol and Philadelphia (2000).
[8] R.E. Waltz, *et al*., Phys. Plasmas **4**, 2482 (1997).
[9] R.E. Waltz, private communication (2002).
[10] M. Erba, *et al*., Plasma Phys. Control. Fusion **39**, 261 (1997).
[11] W.A. Houlberg, *et al.*, Phys. Plasmas **4**, 3230 (1997).
[12] M. Kotschenreuther, Bull. Am. Phys. Soc. **37**, 1432 (1992).
[13] T.S. Hahm and K.H. Burrell, Phys. Plasmas **2**, 1648 (1995).